# Oligomerization-Dependent Changes in the Thermodynamic Properties of the TPR-MET Receptor Tyrosine Kinase†

John L. Hays and Stanley J. Watowich*

*Department of Human Biological Chemistry and Genetics and Sealy Center for Structural Biology, University of Texas Medical Branch, Galveston, Texas 77555-0645*

*Received December 29, 2003; Revised Manuscript Received June 10, 2004*

ABSTRACT: Although oligomerization of receptor tyrosine kinases (RTKs) is necessary for receptor activation and signaling, a quantitative understanding of how oligomerization mediates these critical processes does not exist. We present a comparative thermodynamic analysis of functionally active dimeric and functionally inactive monomeric soluble analogues of the c-MET RTK, which clearly reveal that oligomerization regulates the binding affinity and binding kinetics of the kinase toward ATP and tyrosine-containing peptide substrates. Thermodynamic binding data for oligomeric c-MET were obtained from the dimeric TPR-MET oncoprotein, a functionally active fusion derivative of the c-MET RTK. This naturally occurring oncoprotein contains the cytoplasmic domain of c-MET fused to a coiled coil dimerization domain from the nuclear pore complex. Comparative data were obtained from a soluble monomeric kinase compromising the c-MET cytoplasmic domain (cytoMET). Significantly, under equilibrium binding conditions, the oligomeric phosphorylated kinase showed a significantly lower dissociation constant ($K_{d,dimer} = 11\ \mu M$) for a tyrosine-containing peptide derived from the C-terminal tail of the c-MET RTK when compared to the phosphorylated monomeric kinase cytoMET ($K_{d,monomer} = 140\ \mu M$). Surprisingly, equilibrium dissociation constants measured for the kinase and ATP were independent of the oligomerization state of the kinase ($\sim 10\ \mu M$). Stopped-flow analysis of peptide substrate binding showed that the association rate constants ($k_2$) differed 2-fold and dissociation rate constants ($k_{-2}$) differed 10-fold when phosphorylated TPR-MET was compared to phosphorylated cytoMET. ATP binding abrogated the differences in $k_2$ rates observed between the two oligomeric states of the c-MET cytoplasmic domain. These results clearly imply that oligomerization induces important thermodynamic and conformational changes in the substrate binding regions of the c-MET protein and provide quantitative mechanistic insights into the necessary role of oligomerization in RTK activation.

Binding of extracellular ligand to its cognate receptor tyrosine kinase (RTK)[1] initiates an intracellular signaling cascade that can induce cellular differentiation, proliferation, migration, and other cellular responses (*1*). Ligand binding to a monomeric RTK facilitates receptor oligomerization and subsequent autophosphorylation of tyrosine residues both within a regulatory activation loop and at sites adjacent to the kinase domain (*1*−*5*). Activation loop phosphorylation typically results in increased catalytic activity of the kinase. Phosphorylated tyrosine residues adjacent to the kinase domain act as docking sites for secondary signaling molecules, which typically interact through SH-2 (Src homology 2) or PTB (phosphotyrosine binding) domains. Activation of these secondary signaling molecules, through either phosphorylation or receptor binding, initiates downstream intracellular signaling cascades (*1*, *6*). RTK oligomerization and autophosphorylation are both necessary for efficient receptor activation and signaling, but neither alone is sufficient for full RTK activation (*7*−*10*).

The importance of receptor oligomerization in signaling has been highlighted by numerous observations associating ligand-independent receptor oligomerization with aberrant RTK activation and signaling (*11*). In many cases, constitutively active RTK oncoproteins result from chromosomal translocations that fuse large portions of the RTK cytoplasmic domain to an oligomerization domain (e.g., TPR-MET, TEL-PDGFR, and PTC-1) (*12*−*14*) or point mutations in the extracellular or juxtamembrane domains that promote RTK dimerization (*11*, *15*). Related studies using tyrosine phosphatase inhibitors have demonstrated that while autophosphorylation of both EGFR and PDGFR can be achieved in the absence of extracellular ligand stimulation, these autophosphorylated monomers cannot fully mimic the responses of ligand-stimulated receptors either in whole cells or in *in vitro* preparations (*9*, *16*).

† This work was supported by a grant from the National Library of Medicine (Training Grant 2T15LM07093) and by Grant 4952-052 (to S.J.W.) from the Texas Higher Education Coordinating Board and the Sealy Center for Structural Biology (University of Texas Medical Branch). J.L.H. was supported by a grant from the Keck Center for Computational and Structural Biology, NLM Training Grant 2T15LM07093.

* Address correspondence to this author. Phone: (409) 747-4749. Fax: (409) 747-4745. E-mail: watowich@bloch.utmb.edu.

[1] Abbreviations: AMPPnP, 5′-adenylyl imidodiphosphate; ATP, adenosine 5′-triphosphate; CHAPS, 3-[(3-cholamidopropyl)dimethylammonio]-1-propanesulfonic acid; DTT, dithiothreitol; MANT-AMPPnP, 2′(3′)-*O*-(*N*-methylanthraniloyl)-5′-adenylyl imidodiphosphate; Ni-NTA, nickel nitrilotriacetic acid; RTK, receptor tyrosine kinase.

10.1021/bi0363275 CCC: $27.50 
Published on Web 07/20/2004

The phosphorylation state of RTKs has been studied as an oligomerization-independent regulatory mechanism in RTKs (*12*, *17*−*19*). For example, the angiogenic RTKs Tie-2 and vascular endothelial growth factor receptor 2 (VEGFR-2) showed increased catalytic activity dependent on the phosphorylation state of the receptor. Unfortunately, only the monomeric kinase domain of these proteins was studied; therefore, these results did not address how autophosphorylation modulated the oligomeric receptor (*18*, *19*). Recent work in our laboratory demonstrated that the oligomeric phosphorylated TPR-MET oncoprotein showed a greater than 5-fold increase in the specificity constant ($k_{cat}/K_m$) for ATP and greater than 15-fold increase in the specificity constant for tyrosine-containing peptide substrates when compared to the isolated cytoplasmic domain of the c-MET RTK (cytoMET) (*20*). Recent crystallographic studies have postulated that an interaction might exist between adjacent subunits of the c-Kit RTK cytoplasmic domain (*21*) and between neighboring COOH-terminal regions of the EGF RTK (*22*), although a direct observation of such interactions does not yet exist. Together, these results suggest that while RTK autophosphorylation is an important regulatory mechanism, additional oligomerization-induced changes may necessarily occur to alter the active site conformation and render the RTK fully functional.

Kinetic and thermodynamic characterization of RTKs has previously been performed on isolated kinase domains, whole cytoplasmic domains, or whole receptors. Cheng and Koland showed that the cytoplasmic domain of the EGFR had an almost 10-fold greater $K_d$ for an ATP analogue than a carboxyl-terminal deletion mutant of the cytoplasmic tail (*23*), demonstrating that the isolated kinase domain may not be a sufficient model for RTK function. Additional studies showed that the EGFR carboxy-terminal deletion mutant also had different steady-state catalytic parameters when compared to the whole cytoplasmic domain, and these differences were substrate dependent (*24*). In the insulin receptor (IR), which forms an inactive disulfide-linked dimer in the absence of extracellular ligand, autophosphorylation kinetics were observed to follow a two-phase model where the ligand-activated receptor has a prolonged fast phase compared to the nonligand-stimulated receptor (*25*). These results suggested that conformational changes in the IR occurred upon ligand binding to the extracellular side of the receptor. Quantitative studies of whole receptors have proven difficult due to the complexity of their transmembrane spanning structures. It is clear, however, that a phosphorylated monomeric construct, whether an isolated kinase domain or whole cytoplasmic domain, is not sufficient to completely explain RTK activity. A better model for studying RTKs would allow the quantitative measurement of the relative contribution of autophosphorylation and oligomerization to the activation process.

In this paper we investigated the extent to which oligomerization modulated the thermodynamic properties of the c-MET RTK. To model the active oligomeric c-MET protein, we studied its soluble oncoprotein derivative TPR-MET. The TPR-MET oncoprotein is a fusion of the cytoplasmic domain of the c-MET RTK and a domain from the nuclear pore complex (*12*, *26*, *27*). The fusion results in the loss of the extracellular, transmembrane, and a portion of the juxtamembrane domains of c-MET and their replacement with a leucine zipper dimerization domain. The resulting fusion protein is a constitutively active phosphorylated dimer that is oligomerized through the TPR domain, as demonstrated by site-directed mutagenesis (*12*). This oncoprotein could transform NIH-3T3 cells independent of extracellular ligand stimulation (*12*) and had the ability to produce mammary hyperplasia and carcinoma as well as multiple other neoplasms in transgenic mice (*28*). TPR-MET and the ligand-activated c-MET receptor have been shown to be similarly phosphorylated and to signal through similar pathways both *in vivo* and in cell culture (*29*, *30*−*32*). CytoMET is the cytoplasmic domain of the c-MET RTK, homologous to TPR-MET but lacking the leucine zipper TPR region. Although this protein had kinase activity, it could not transform NIH3T3 cells and was, therefore, functionally inactive (*12*). These studies suggested that there are differences between functionally active TPR-MET and functionally inactive cytoMET. Here we present a detailed analysis that conclusively shows phosphorylated TPR-MET and phosphorylated cytoMET have significantly different thermodynamic properties. Since these two proteins differ only in their oligomerization state, this implies that their thermodynamic properties were modulated by oligomerization-induced conformational changes and that similar oligomerization-induced conformational changes likely are associated with c-MET activation.

## EXPERIMENTAL PROCEDURES

*Materials*. Adenosine 5′-triphosphate (ATP) and 5′-adenylyl imidodiphosphate (AMPPnP) were purchased from Sigma. The Bac-to-Bac baculovirus expression system, SF-900II SFM, fetal bovine serum (FBS), and 100× antibiotic/antimycotic were purchased from Invitrogen. Complete protease inhibitor cocktail was purchased from Boehringer Mannheim. 2′(3′)-*O*-(*N*-methylanthraniloyl)-5′-adenylyl imidodiphosphate (MANT-AMPPnP) was synthesized by the UTMB Synthetic Organic Chemistry Core Laboratory according to Hiratsuka (*33*). Fluorescently labeled PepTyr489 (NBD-DSDVHVNAT**Y**VNVKCVAP) was synthesized and purified in the UTMB Protein Chemistry Core Facility and its identity verified by mass spectroscopy. Anti-human c-Met antibody was purchased from Santa Cruz Biotechnology (sc-161); anti-phosphotyrosine (clone 4G10) and the anti-phosphorylated MET activation loop antibodies were from Upstate Biotechnology.

*Protein Purification*. Expression and purification of full-length TPR-MET and the cytoplasmic domain of the c-MET receptor (cytoMET) were described in detail elsewhere (*20*). Briefly, both proteins were cloned into the Bac-to-Bac baculovirus expression system (Invitrogen) with a C-terminal hexahistidine tag. Recombinant baculovirus was used to infect Sf-9 insect cells at a multiplicity of infection (MOI) of 5. Cells were harvested after 72 h and lysed in TBSC lysis buffer (50 mM Tris, pH 7.5, 150 mM NaCl, 0.5% CHAPS) supplemented with 1 mM DTT and 1× complete protease inhibitor cocktail. TPR-MET and cytoMET were separately purified from the cleared lysate by binding and elution from Ni-NTA beads (Qiagen). Purified protein was dialyzed into PBSC (50 mM sodium phosphate, pH 6.5, 150 mM NaCl, 0.5% CHAPS, 1 mM DTT) supplemented with 50 $\mu$M ATP, 25 mM $MgCl_2$, and 5 mM $MnCl_2$ to ensure complete autophosphorylation. Both proteins were recognized

by a commercially available anti-human c-MET antibody (Santa Cruz, SC-161) that was derived from a peptide corresponding to the carboxy-terminal residues of c-MET. Both TPR-MET and cytoMET are phosphorylated to similar extents and on similar tyrosine residues as demonstrated from their recognition by anti-phosphotyrosine antibody 4G10 (Upstate Biotechnology) and separate antibodies specific for the phosphorylated activation loop and the carboxy-terminal phosphotyrosine site 1365 of c-MET (Upstate Biotechnology) (data not shown). Furthermore, incubation of this phosphorylated enzyme with [$\gamma$-$^{32}$P]ATP revealed no further incorporation of phosphate into either TPR-MET or cytoMET, indicating that both enzymes were maximally autophosphorylated. As judged by Western blot quantification, no change in phosphotyrosine levels was observed for either cytoMET or TPR-MET during the course of the experiments (data not shown). Excess ATP, ADP, $MgCl_2$, and $MnCl_2$ were removed from purified proteins by successive dialysis into PBSC and the proteins stored at 4 °C.

*Equilibrium Binding Studies of TPR-MET and CytoMET*. Binding of MANT-AMPPnP, ATP, and fluorescent-labeled tyrosine-containing peptide (PepTyr489) to purified TPR-MET and cytoMET was measured using a Fluorolog-3 spectrofluorometer (Model FL3-22; Jobin-Yvon) with dual grating monochromators on both the excitation and emission pathways. Quenching of the fluorescence from the five common tryptophan residues found in both TPR-MET and cytoMET was measured at increasing concentrations of substrate. Reactions were performed in PBSC supplemented with 5 mM DTT. In peptide binding reactions, 1% DMSO was included in the reaction buffer. In reactions with MANT-AMPPnP or AMPPnP, the reaction buffer was supplemented with 5 mM $MgCl_2$. All data were collected at 10 °C with an excitation wavelength ($\lambda^{ex}$) of 290 nm and emission monitored from 300 to 387 nm for MANT-AMPPnP binding and from 300 to 400 nm for peptide binding. Both the sample and a reference cuvette with buffer and ligand were recorded. Fluorescence was corrected for inner filter effects by measuring the absorbance of the protein/ligand solutions at the excitation and emission wavelengths. The quenching of tryptophan fluorescence occurring upon the addition of substrate to a constant amount of protein was assumed to be proportional to the amount of protein-bound substrate present. The data were fitted using the following equation to obtain dissociation constants:

$$\Delta F/F^0 = 1 - \{Q[\text{substrate}]/(K_d + [\text{substrate}])\}$$

where $\Delta F$ represents the fluorescence of the sample minus the background cuvette, $F^0$ is the initial protein fluorescence in the absence of ligand, $Q$ is the maximum quenching of the protein during the experiment, and $K_d$ is the dissociation constant (*34*). The data were plotted as $\Delta F/F^0$ vs [substrate] and fit using nonlinear least squares regression analysis to the above equation with the Graphpad Prism program and $K_d$ and $Q$ as fitting parameters.

*Stopped-Flow Fluorescence Measurements*. All stopped-flow measurements were performed on a Fluorolog-3 spectrofluorometer as described above, with a $\mu$-flow stopped-flow attachment (Jobin-Yvon). Samples were mixed in equal volumes, and fluorescent changes were monitored at a $\lambda^{ex}$ of 290 nm (1 nm slits) and an emission wavelength ($\lambda^{em}$) of 335 nm (10 nm slits) with dual grating monochromators on both the excitation and emission sides. Buffers used were identical to those described for equilibrium binding measurements. Time-dependent emission quenching was collected for a total of 100−300 s with 0.005−0.1 s increments. Three to five data sets were recorded for each concentration of ligand at a fixed concentration of protein. The data were analyzed using nonlinear least squares regression in the Graphpad Prism program and fit to a two-phase exponential decay:

$$Y = \text{spanA} \times e^{-k_a t} + \text{spanB} \times e^{-k_{obs} t} + \text{plateau}$$

where spanA and spanB correspond to the amplitude of the exponential process, $k_a$ is the photobleaching-associated rate constant, $k_{obs}$ is the observed pseudo-first-order rate constant, and plateau is the fluorescence at $t = \infty$. The observed photobleaching rate constant was measured in the absence of ligands. The measured $k_{obs}$ vs [substrate] were fit with least squares linear regression analysis in the Graphpad Prism and yielded straight lines with slopes corresponding to $k_{on}$ and intercepts that correspond to $k_{off}$ for the selected substrate (*34*).

## RESULTS

*Quenching of Intrinsic Tryptophan Fluorescence in TPR-MET and CytoMET*. We have previously shown that both TPR-MET and cytoMET are catalytically active against a biotinylated peptide that corresponded to Tyr-489 (residue 1356 in c-MET) in the C-terminal tail of the TPR-MET oncoprotein (PepTyr489) (*20*). This tyrosine residue is crucial for cellular signaling by both c-MET and TPR-MET (*30*). In addition, quenching of the tryptophan residues found within the TPR-MET and cytoMET by MANT-AMPPnP alone has been described (*20*). In this paper we significantly extend these results by determining peptide equilibrium binding constants and preequilibrium rates and the degree of allosteric interaction between the peptide and ATP binding sites in the different oligomeric states of the c-MET receptor.

Four of the five tryptophan residues found in TPR-MET and cytoMET are within the carboxy-terminal kinase domain and also within 20 Å of the peptide binding site, as determined by sequence analysis and comparison with the known structure of the insulin receptor (*35*). Therefore, a fixed amount of protein (0.01−3 $\mu$M) was titrated with increasing amounts of substrate, and the change in intrinsic tryptophan fluorescence was measured over the range of the emission peak. The area under the curve was integrated, inner filter effects were subtracted out, and normalized fluorescence was plotted against substrate concentration. These data were fit using nonlinear least squares regression analysis (Figures 1 and 2). Since dimeric TPR-MET has two binding sites for both ATP and peptide ligand, it was important to determine if there was any quenching of tryptophan residues in one subunit by binding of either ATP or peptide to the other, which might lead to a nonlinear signal change. To determine if there was fluorescent energy exchange interactions between the subunits of the TPR-MET dimer, the experiment was repeated using a greater than 30-fold difference in protein concentrations (up to 3 $\mu$M). No changes in fitting parameters were needed to accurately fit the data over the range of protein concentrations tried. Thus, binding

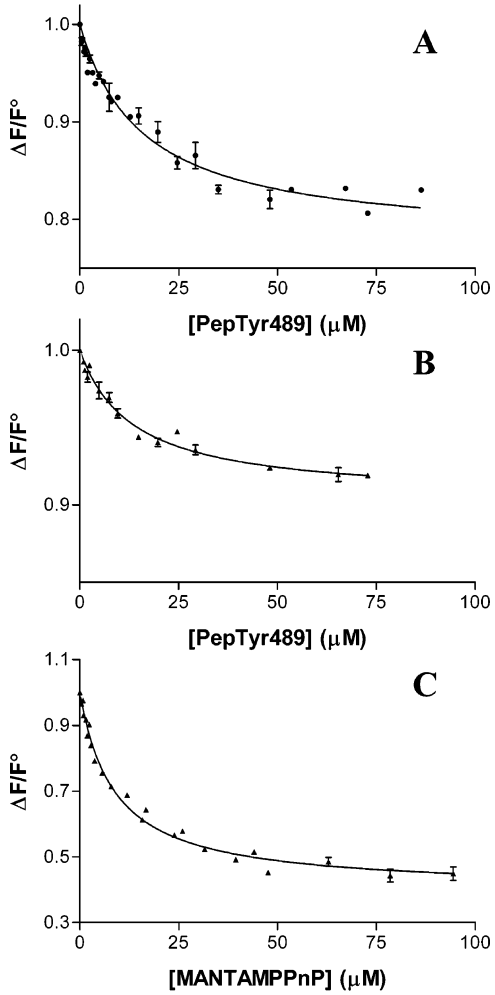


FIGURE 1: Equilibrium binding of MANT-AMPPnP and PepTyr489 to TPR-MET. Panels A−C show plots of normalized fluorescence relative to initial fluorescence at the indicated concentrations of substrate. Panel A: PepTyr489. Panel B: PepTyr489 + 150 $\mu$M AMPPnP. Panel C: MANT-AMPPnP + 120 $\mu$M PepTyr489.

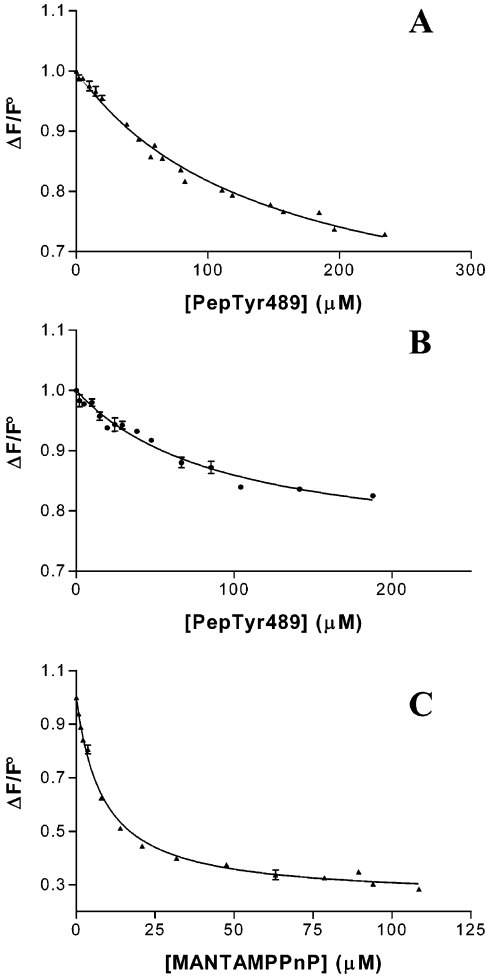


FIGURE 2: Equilibrium binding of MANT-AMPPnP and PepTyr489 to cytoMET. Panels A−C show plots of normalized fluorescence relative to initial fluorescence at the indicated concentrations of substrate. Panel A: PepTyr489. Panel B: PepTyr489 + 150 $\mu$M AMPPnP. Panel C: MANT-AMPPnP + 250 $\mu$M PepTyr489.

of the first ligand to the protein quenches either all of the fluorescence or the same amount of fluorescence as binding of the second ligand (data not shown).

Table 1 summarizes the equilibrium binding data obtained from analysis of Figures 1 and 2. In previous work, we described the binding of AMPPnP, a nonhydrolyzable derivative of ATP, and its fluorescent analogue MANT-AMPPnP to both phosphorylated TPR-MET and phosphorylated cytoMET (*20*). Importantly, oligomerization produced a 3-fold decrease in the dissociation constant between AMPPnP and phosphorylated TPR-MET when compared to AMPPnP and phosphorylated cytoMET. Also, there was no significant difference between the binding of MANT-AMPPnP and AMPPnP for either protein, and therefore, MANT-AMPPnP could be used to accurately measure the binding of AMPPnP to either protein. The binding constants for PepTyr489 ($K_{d,pep}$) were 13.4 and 143.4 $\mu$M for phosphorylated TPR-MET and phosphorylated cytoMET, respectively.

We investigated the degree of allosteric interactions between peptide and ATP binding sites in both phosphorylated TPR-MET and phosphorylated cytoMET. The presence of excess AMPPnP (150 $\mu$M) did not alter the binding affinity between PepTyr489 and phosphorylated TPR-MET ($K_{d,pepATP}$ = 15.9 $\mu$M). However, the binding affinity between PepTyr489 and phosphorylated cytoMET was significantly decreased in the presence of excess AMPPnP ($K_{d,pepATP}$ =

Table 1: Equilibrium Binding of TPR-MET and CytoMet[a]

| | $K_d$ (±SE)[b] ($\mu$M) | | | |
|---|---|---|---|---|
| | AMPPnP[c] | PepTyr489 | PepTyr489 + satd AMPPnP | MANT-AMPPnP + satd PepTyr489 |
| TPR-MET | 5.7 (0.58) | 13.4 (1.4) | 15.9 (1.9) | 8.7 (0.58) |
| cytoMET | 17.5 (1.9) | 143.4 (12.9) | 93.9 (13.5) | 8.5 (0.7) |
| *p*-value | 0.02 | <0.001 | <0.001 | 0.004 |
| | $\Delta G$ (±SE)[b] (kJ) | | | |
| | AMPPnP[c] | PepTyr489 | PepTyr489 + satd AMPPnP | MANT-AMPPnP + satd PepTyr489 |
| TPR-MET | 28.4 (2. 9) | 26.4 (2.7) | 25.9 (3.1) | 27.4 (1.8) |
| cytoMET | 25.7 (2.8) | 20.8 (1.9) | 21.8 (3.1) | 27.5 (2.2) |

[a] TPR-MET and cytoMET were analyzed following protocols in Experimental Procedures. The $K_d$ values reported represent the $K_d$ ± SE for unweighted nonlinear least squares regression analysis of data from Figures 1 and 2. Free energy interactions between the protein and substrate were calculated using $\Delta G = -RT \ln(K_d)$. Two-tailed *p*-values were calculated within the Graphpad Prism program using paired *t*-tests. [b] Standard error. [c] From ref *20*.

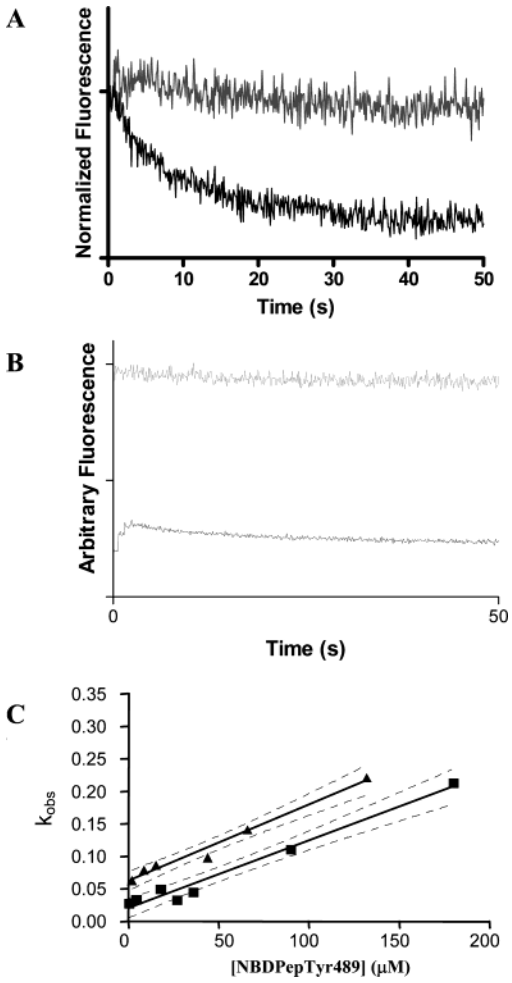


FIGURE 3: Stopped-flow analysis of TPR-MET. Time-based quenching (10 ms resolution) of intrinsic tryptophan fluorescence from TPR-MET by either PepTyr489 (panel A) or MANT-AMPPnP (panel B). The top trace in both panel A and panel B is TPR-MET with no ligand. The bottom trace represents TPR-MET mixed with 90 $\mu$M PepTyr489 (final concentration after mixing) in panel A or 20 $\mu$M MANT-AMPPnP (final concentration after mixing) in panel B. Data are an average of at least three individual scans and fit with a double exponential decay as described in Experimental Procedures to obtain $k_{obs}$. Panel C represents $k_{obs}$ obtained at various concentrations of PepTyr489: TPR-MET with PepTyr489 (■) and TPR-MET preincubated with AMPPnP prior to mixing with PepTyr489 (▲). Dashed lines represent 95% confidence intervals for the linear regression analysis.

93.9 $\mu$M). The converse was not true, as binding of MANT-AMPPnP was not significantly affected by the presence of excess PepTyr489 in either TPR-MET or cytoMET (Table 1). The values of $K_{d,pepATP}$ for both enzymes were similar to those reported for the $K_m$ values for both enzymes (*20*), which would indicate that the catalytic step in the reaction has a rate that is very small in comparison with the dissociation constants. These results demonstrated a statistically significant difference in the peptide dissociation constant between phosphorylated TPR-MET and phosphorylated cytoMET and that the ATP binding site of the kinase was largely independent of the oligomerization-induced changes that were present within the peptide binding region.

*Stopped-Flow Analysis of Substrate Binding to TPR-MET and CytoMET*. Stopped-flow analysis of both TPR-MET and cytoMET with MANT-AMPPnP and PepTyr489 was undertaken to determine preequilibrium kinetic behavior for

Scheme 1

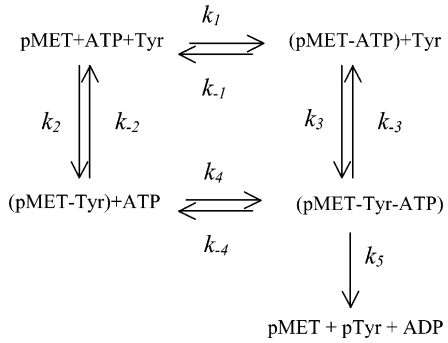


both ligands under pseudo-first-order conditions with an excess of ligand with respect to protein. The quenching of the emission peak at 335 nm was followed upon excitation at 290 nm in 5−100 ms time increments for 100−300 s. Figure 3A shows a typical time-dependent spectrum for the association of PepTyr489 with TPR-MET. The entire quenching amplitude was traceable from the initial protein equilibrium fluorescence value (in the absence of ligand) to an equilibrium value in the presence of ligand. Similar results were obtained when measuring the quenching from PepTyr489 in the presence of saturating amounts of AMPPnP. The quenching curves were fit with double exponential decay functions ($Y = \text{spanA} \times e^{-k_a t} + \text{spanB} \times e^{-k_{obs} t} + \text{plateau}$). The first term ($\text{spanA} \times e^{-k_a t}$) described the nonspecific quenching that can be measured in the absence of ligand. The second term ($\text{spanB} \times e^{-k_{obs} t}$) represented the quenching due to preequilibrium mixing of the protein with ligand. Plateau is the equilibrium fluorescence of the protein plus ligand mixture. All rate constants refer to Scheme 1 for the position in the reaction scheme.

All time-dependent fluorescence data collected for a range of PepTyr489 concentrations fit the double exponential function. In contrast, attempted fitting of the data with single-exponential functions yielded systematic deviations that could be observed in the residual analysis. Plots of $k_{obs}$ vs [PepTyr489] are shown in Figures 3C and 4C for TPR-MET and cytoMET, respectively. Both proteins showed a linear response with respect to increasing peptide concentration, and linear regression analysis revealed a pseudo-first-order association constant $k_2 = 0.0010\ s^{-1}$ for TPR-MET and peptide. This value did not change significantly if AMPPnP was initially bound to TPR-MET and was measured as $k_4 = 0.0012\ s^{-1}$ (Table 2). For cytoMET, analysis of the time-dependent fluorescence data provided a pseudo-first-order association constant $k_2 = 0.00053$, approximately 2-fold slower than the $k_2$ value measured for TPR-MET. Binding of AMPPnP to cytoMET prior to stopped-flow analysis with PepTyr489 significantly increased the onrate for PepTyr489 to cytoMET by ~3-fold to $k_4 = 0.0015$. This value was statistically identical to the measured onrate of peptide to TPR-MET. Similarly, measured offrates indicated that peptide ligand dissociated from monomeric cytoMET with a $k_{-2} = 0.177\ s^{-1}$, which was ~10 times faster than the measured dissociation rate from dimeric TPR-MET, $k_{-2} = 0.019\ s^{-1}$. No significant differences in peptide dissociation rates were observed when the kinases were in excess AMPPnP, as $k_{-3} = 0.10\ s^{-1}$ for cytoMET and $k_{-3} = 0.061\ s^{-1}$ for TPR-MET (Table 2). These results support our above model that there are significant differences between the monomeric cytoMET

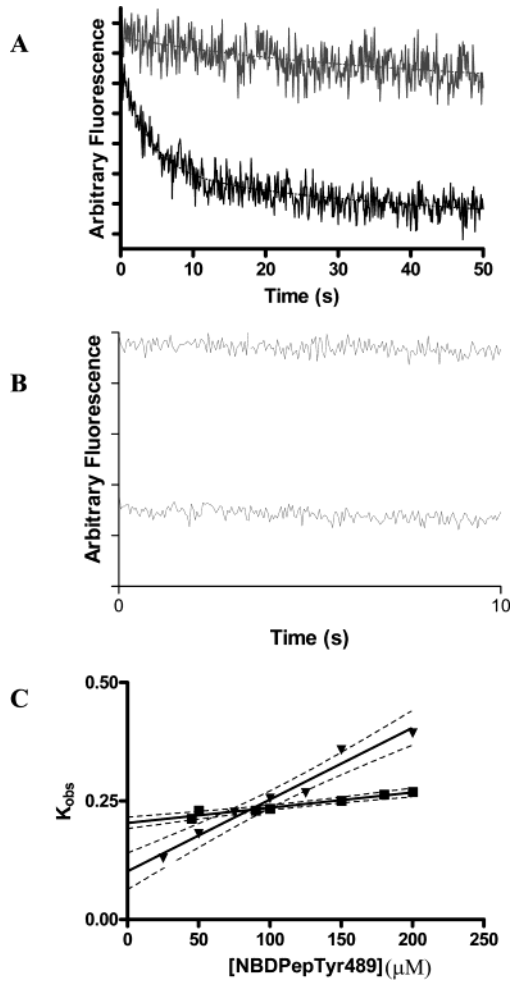


FIGURE 4: Stopped-flow analysis of cytoMET. Time-based quenching (10 ms resolution) of intrinsic tryptophan fluorescence from cytoMET by either PepTyr489 (panel A) or MANT-AMPPnP (panel B). The top trace in both panel A and panel B is cytoMET with no ligand. The bottom trace represents cytoMET mixed with 180 $\mu$M PepTyr489 (final concentration after mixing) in panel A or 40 $\mu$M MANT-AMPPnP (final concentration after mixing) in panel B. Data are an average of at least three individual scans and fit with a double exponential decay as described in Experimental Procedures to obtain $k_{obs}$. Panel C represents $k_{obs}$ obtained at various concentrations of PepTyr489: cytoMET with PepTyr489 (■) and cytoMET preincubated with AMPPnP prior to mixing with PepTyr489 (▼). Dashed lines represent 95% confidence intervals for the linear regression analysis.

and the dimeric TPR-MET in conformation of their respective peptide binding regions, and these differences were likely reduced upon binding of AMPPnP prior to binding of peptide.

For TPR-MET, the value of $k_{-2}/k_2$, the pre-steady-state interaction between peptide and enzyme in the absence of AMPPnP, yielded a calculated dissociation constant that was very similar to the measured dissociation constant. When considering the binding of peptide to the AMPPnP·TPR-MET complex, the ratio of $k_{-3}/k_3$ overestimated the dissociation constant by approximately 3-fold. However, independently constraining the values of $k_{on}$ and $k_{off}$ with the value of the measured $K_d$ in the linear regression analysis did not yield statistically significant differences in the $k_{-3}$ or $k_3$ values. In the case of cytoMET, binding of peptide in the absence of AMPPnP showed an approximate 2-fold increase between the $k_{-2}/k_2$ ratio and the equilibrium binding measurements, while in the presence of AMPPnP, the $k_{-3}/k_3$ ratio was similar to the equilibrium dissociation constant describing that step. Similar to TPR-MET, independently constraining the fitting parameters in the linear regression analysis with the equilibrium binding constant yielded statistically identical values to the unconstrained data. Since the ratio of on/off rates so closely agrees with the measured dissociation constants, this indicates that a single-step process is occurring upon ligand binding. Binding of a ligand may not structurally alter the protein significantly but may account for the quenching of the tryptophan fluorescence, or ligand-induced structural alterations may occur in the kinase domain that account for the quenching of the tryptophan fluorescence, or both may occur on a similar time scale so that their respective signals are combined to form the measured single response.

Previous work has shown that MANT-AMPPnP and AMPPnP bind similarly to TPR-MET and cytoMET (*20*). Time-dependent quenching of TPR-MET by MANT-AMPPnP was performed as above for analysis of peptide binding, but only a minor part (<10%) of the overall equilibrium quenching was able to be observed at any given concentration of MANT-AMPPnP. The instrument dead time was determined to be 4 ms (data not shown), and this would imply that 90% of the quenching amplitude occurred within the instrument dead time (Figures 3B and 4B). In an attempt to slow the kinetic process into an observable time scale, similar experiments with other concentrations of MANT-AMPPnP and 10-fold lower concentrations of protein were tested but yielded similar results (data not shown). These results implied a fast association step between ATP and kinase with a half-life of <4 ms, which is in agreement with other groups who observed that MANT-ATP bound to kinases with a half-life of ~2 ms (*36*).

## DISCUSSION

Many groups have demonstrated the importance of RTKs in both normal and diseased tissues (*1*, *3*, *4*). Although the mechanism and pathways RTKs use to initiate and propagate intracellular signals have been exhaustively researched, little is known about the detailed molecular basis of RTK activation and what is necessary and sufficient for receptor activation and signaling. To study the effect of oligomerization on modulating receptor tyrosine kinase activity, we have used TPR-MET, a functionally active oligomeric protein derived from the cytoplasmic domain of the c-MET receptor and compared it to a functionally inactive monomeric protein encapsulating the cytoplasmic domain of the c-MET receptor (*12*). Previous work has demonstrated a significant difference in the catalytic activity of the two proteins (*20*), and in this work we show differences in their thermodynamic properties as well.

The equilibrium dissociation constants for peptide and nucleotide ligands have been measured for the monomeric and oligomeric states of the c-MET protein. Additionally, the cooperativity between peptide and nucleotide ligand binding was addressed. Significantly, receptor oligomerization increased the affinity of the kinase for tyrosine-containing peptide substrates by greater than 1 order of magnitude. In addition, binding of peptide ligand in the presence of saturating amounts of AMPPnP still leads to an

Table 2: Preequilibrium Binding Kinetics of TPR-MET and CytoMet[a]

| | $k$ (±SE) ($s^{-1}$) | | | |
|---|---|---|---|---|
| | PepTyr489 | | PepTyr489 + satd AMPPnP | |
| | $k_{on}$ | $k_{off}$ | $k_{on}$ | $k_{off}$ |
| TPR-MET | $1.0 \times 10^{-3}$ ($7.0 \times 10^{-5}$) | 0.019 ($6.0 \times 10^{-3}$) | $1.2 \times 10^{-3}$ ($1 \times 10^{-4}$) | 0.061 (0.011) |
| cytoMET | $5.3 \times 10^{-4}$ ($3.0 \times 10^{-5}$) | 0.17 ($4.0 \times 10^{-3}$) | $1.5 \times 10^{-3}$ ($1.2 \times 10^{-4}$) | 0.10 (0.015) |

[a] TPR-MET and cytoMET were analyzed following protocols in Experimental Procedures. The $k_{on}$ and $k_{off}$ values were calculated from $k_{obs}$ ± SE values representing the unweighted nonlinear least squares regression analysis of data from Figures 3 and 4 for $k_{obs}$ values. $k_{on}$ and $k_{off}$ rates were calculated from least squares linear regression analysis of data from Figures 3D and 4D.

~6-fold difference between TPR-MET and cytoMET (Table 1). This strongly implies that receptor oligomerization modifies the peptide binding site independent of bound nucleotide. Conversely, oligomerization had very little effect on the binding of nucleotide to the kinase domain independent of whether a tyrosine-containing peptide is bound to the receptor.

It is expected that if Scheme 1 is a valid, closed thermodynamic cycle, the sum of the free energies associated with each individual step as you choose a path around the cycle must be equal to the sum along any other pathway. For example, $\Delta G_1 + \Delta G_3 = \Delta G_2 + \Delta G_4$ [where $\Delta G_n = -RT \ln(k_n)$]. Calculating the $\Delta G$ associated with each step (Table 1) and attempting to close the thermodynamic cycle yield very good agreement between the two possible pathways for each protein. For TPR-MET, $\Delta G_1 \Delta G_3 = 54.3$ kJ, and $\Delta G_2 \Delta G_4 = 53.8$ kJ. Similarly, for cytoMET, $\Delta G_1 \Delta G_3 = 47.5$ kJ and $\Delta G_2 \Delta G_4 = 48.3$ kJ.

Other groups have measured the affinity of various kinases for ATP and its fluorescent derivatives, as well as for various tyrosine-containing substrates (*23*, *36*−*38*). Results for ATP and the various nucleotide derivatives are consistent among the many kinases, with $K_d$ measurements ranging from 1 to 40 $\mu$M. These values were consistent with ATP binding affinities to TPR-MET and cytoMET. In contrast, kinases show a greater diversity in their affinities for peptide substrates, with $K_d$ values ranging from 1 $\mu$M to >2 mM. Our measured affinities between peptide substrates and kinase species were within the higher affinity (i.e., tighter binding) end of this range.

In our studies, we used a peptide derived from the C-terminal tail of the c-MET receptor that has been shown to be phosphorylated in vivo and in vitro (*20*, *39*, *40*). A similar peptide sequence, corresponding to the same tyrosine residue, has been shown to inhibit c-MET receptor activity in the cell culture (*41*). We find the $K_{d,pep}$ to be similar to the $K_{d,ATP}$ for the phosphorylated dimer. This is significant since other groups have argued that nucleotide release is the rate-limiting step in the catalytic mechanism due to a relatively low affinity for peptide substrates (*38*). While this assumption may hold true for monomeric RTK kinase domains and nonspecific peptide ligands, it is definitely not the case for dimeric receptors.

On the basis of relative monomer orientations observed in recent crystallographic structures (*21*, *22*), it has been postulated that intradimer interactions might occur within some RTKs. A possible outcome of intradimer interactions could be stabilization of the kinase activation loop in the dimer, a position that favors peptide binding and catalysis. In the soluble kinase domain of the apoinsulin receptor, the activation loop conformation appeared to block binding of the peptide substrate and ATP in the nonphosphorylated kinase. In contrast, in the structures of ligands complexed to phosphorylated kinase domains the activation loop flips out of the binding site and into an open conformation. In addition, Hubbard et al. (*3*) postulated that the loop was very flexible since both the nonphosphorylated and phosphorylated structures have high *B*-factors within this region. These observations led to two competing hypotheses: (1) oligomerization-induced stabilization of the activation loop in an open conformation leading to an increased $k_{on}$ coupled with an increased affinity for the peptide substrates or (2) no difference in equilibrium dissociation constants between monomer and dimer due to similar increases in the $k_{on}$ and $k_{off}$ rates for the dimeric molecule relative to the monomer. Surprisingly, our model does not support either hypothesis as we clearly observed only small differences in $k_{on}$ and significant decrease in the $k_{off}$ rates for the interaction between peptide and dimer. These measurements suggest that the peptide binding sites were similar for both the monomeric and dimeric phosphorylated apoenzymes, but structural changes occurred following peptide binding that stabilized the peptide binding site in the dimeric enzyme relative to the monomeric enzyme. Thus, oligomerization results in significantly higher affinities between peptide substrates and kinases, and this thermodynamic phenomenon is largely a consequence of differences in peptide $k_{off}$ rates.

Another possible mechanism for RTK activation was that dimerization increased the local concentration of tyrosine-containing substrates available from subunit interactions within the dimer or from exogenous substrate binding through SH2 domains, and this would yield increased kinase activity. While our data cannot specifically discount this argument, we observed that oligomerization changed the inherent thermodynamic properties of the receptor kinase, a result that is not predicted in the local concentration increase hypothesis. It is possible that a complete model of RTK activation may ultimately incorporate increased local concentration effects as well as the measured oligomerization-dependent thermodynamic and kinetic changes reported in this paper.

While equilibrium fluorescent measurements provide dissociation constants for ATP and peptide substrates, they do not provide a mechanism for the kinase reaction. Other groups have characterized the pre-steady-state binding parameters of fluorescent ATP analogues and ADP in attempts to understand the reaction mechanisms of tyrosine kinases (*36*, *38*). Previous kinetic results showed that $k_5$ was the rate-limiting step for the TPR-MET and cytoMET kinases (*20*). However, those studies did not differentiate between the actual catalytic phosphoryl transfer step and product release. Since ATP concentrations within a cell are consider-

ably higher than those needed to saturate the enzyme completely and the observed $k_{on}$ rates for MANT-AMPPnP in this and other studies (*36*, *38*) were significantly higher than the observed $k_{on}$ rates for peptide substrate, it is likely that both monomeric cytoMET and dimeric TPR-MET bind nucleotide before interacting with peptide substrate (E ↔ E·ATP ↔ E·ATP·peptide pathway, Scheme 1). If there were an excess of enzyme and not ATP, it is likely that the reaction flux through the previous pathway as well as the alternative (E ↔ E·peptide ↔ E·ATP·peptide) would be more equal.

RTKs oligomerize in response to ligand binding, and this process facilitates autophosphorylation of the receptor on specific tyrosine residues (*4*). The question remains, does receptor oligomerization modulate the intrinsic autophosphorylation activity, the activity of the enzyme toward downstream signaling molecules, or the intrinsic thermodynamic properties of the receptor? Many groups have studied isolated kinase domains and intracellular regions of RTKs, and their work demonstrates that isolated kinase domains are sufficient for enzymatic activity in vitro (*18*−*20*, *42*). While these domains may be sufficient to study activity in vitro, they do not represent a good model for the functionally active oligomeric RTK. Although TPR-MET dimerization may not exactly mimic the activated c-MET receptor in that TPR-MET is constitutively active and is not membrane-bound, substantial evidence has shown the naturally occurring TPR-MET to be active in cell culture and in vivo utilizing similar signaling pathways to those utilized by the ligand-activated c-MET receptor (*28*−*30*).

On the basis of our reported results (this paper and ref *20*) we propose the following RTK activation mechanism that explains the known thermodynamic and kinetic data. Functionally inactive, or monomeric, receptor resides at the cell membrane with ATP bound. Since this receptor has basal kinase activity, some small degree of autophosphorylation continually occurs; however, no phosphorylated receptor accumulates in the cells due to the action of phosphatases. In support of this mechanistic step, autophosphorylated monomeric species have been observed in cultured cell lines incubated with phosphatase inhibitors (*9*, *16*). Extracellular ligand stimulation promotes oligomerization of the receptor, which results in increased cellular concentrations of autophosphorylated receptor and phosphorylated downstream signaling molecules. The increased accumulations of phosphorylated species are due to several concerted factors: an increase in the kinetic activity of the nonphosphorylated oligomer when compared to the nonphosphorylated monomer (*10*, *25*, *39*), protection of the oligomeric RTK from phosphatase activity (*43*), an increased affinity for substrates by the oligomeric receptor when compared to the monomeric receptor, an increase in the kinase activity of the phosphorylated oligomer when compared to the phosphorylated monomer (*20*), and oligomerization-induced local increases in substrate concentration. The activated receptor is then able to recruit second messengers and activate various signaling cascades until it is inactivated either through internalization, degradation, or inactivation through growth factor release and dephosphorylation. Detailed quantitative models will be necessary to fully appreciate the relative importance of these oligomerization-dependent changes in RTK kinetic and thermodynamic properties. Moreover, the design of therapeutics to counter the oncogenic effects of RTKs must take into account the relative affinities for both ATP and tyrosine-containing substrates as well as the difference in affinities between the activated, oligomeric receptor and the inactive, monomeric receptor.

## ACKNOWLEDGMENT

We thank Dr. D. W. Bolen and Dr. W. Bujalowski for helpful discussions and Dr. M. Park for providing the *tpr-met* clone.

## REFERENCES

1. Schlessinger, J. (2000) Cell Signaling by Receptor Tyrosine Kinases, *Cell 103*, 211−225.
2. Ullrich, A., and Schlessinger, J. (1990) Signal Transduction by Receptors with Tyrosine Kinase Activity, *Cell 61*, 203−212.
3. Hubbard, S. R., Mohammedi, M., and Schlessinger, J. (1998) Autoregulatory Mechanisms in Protein-Tyrosine Kinases, *J. Biol. Chem. 273*, 11987−11990.
4. Weiss, A., and Schlessinger, J (1998) Switching Receptors On or Off by Receptor Dimerization, *Cell 94*, 277−280.
5. Hubbard, S. R., and Hill, J. T. (2000) Protein Tyrosine Kinase Structure and Function, *Annu. Rev. Biochem. 69*, 373−398.
6. Cohen, G. B., Ren, R., and Baltimore, D. (1995) Modular Binding Domains in Signal Transduction Proteins, *Cell 80*, 237−248.
7. Ellis, E. C., Morgan, D. O., Edery, M., Roth, R. A., and Rutter, W. J. (1986) Replacement of Insulin Receptor Tyrosine Residues 1162 and 1163 Compromises Insulin-stimulated Kinase Activity and Uptake of 2-Deoxyglucose, *Cell 45*, 721−732.
8. Longati, P., Bardelli, A., Ponzetto, C., Naldini, L., and Comoglio, P.M. (1994) Tyrosines1234−1235 are Critical for Activation of the Tyrosine Kinase Encoded by the Met Proto-Oncogene (HGF Receptor), *Oncogene 9*, 49−57.
9. Baxter, R. M., Secrist, J. P., Vaillancourt, R. R., and Kazlauskas, A. (1998) Full Activation of the Platelet-derived Growth Factor−Receptor Kinase Involves Multiple Events, *J. Biol. Chem. 273*, 17050−17055.
10. Baer, K., Al-Hasani, H., Parvaresch, S., Corona, T., Rufer, A., Nolle, V., Bergschneider, E., and Klein, H. W. (2001) Dimerization Induced Activation of Soluble Insulin/IGF-1 Receptor Kinases: An Alternative Mechanism of Activation, *Biochemistry 40*, 14268−14278.
11. Watowich, S. S., Yoshimura, A., Longmore, G. D., Hilton, D. J., Yoshimura, Y., and Lodish, H. F. (1992) Homodimerization and Constitutive Activation of the Erythropoietin Receptor, *Proc. Natl. Acad. Sci. U.S.A. 89*, 2140−2144.
12. Rodrigues, G. A., and Park, M. (1993) Dimerization Mediated through a Leucine Zipper Activates the Oncogenic Potential of the *met* Receptor Tyrosine Kinase, *Mol. Cell. Biol. 13*, 6711−6722.
13. Golub, T. R., Barker, G. F., Lovett, M., and Gilliland, D. G. (1994) Fusion of PDGF Receptor Beta to a Novel ETS-like Gene, *tel*, in Chronic Myelomonocytic Leukeia with t(5;12) Chromosomal Translocation, *Cell 77*, 307−316.
14. Tong, Q., Xing, S., and Jhiang, S. M. (1997) Leucine Zipper-mediated Dimerization is Essential for the PTC1 Oncogenic Activity, *J. Biol. Chem. 272*, 9043−9047.
15. Hunter, T. (1997) Oncoprotein Networks, *Cell 88*, 333−346.
16. Posner, B. I., Faure, R., Burgess, J., Bevan, A. P., Lachance, D., Zhang-sun, G., Fantus, I., Ng, J. B., Hall, D. A., Lum, B. S., and Shaver, A. (1994) Peroxovanadium Compounds. A New Class of Potent Phosphotyrosine Phosphatase Inhibitors Which are Insulin Mimetics, *J. Biol. Chem. 269*, 4596−4604.
17. Posner, I., Engel, M., and Levitzki A. (1992) Kinetic Model of the Epidermal Growth Factor (EGF) Receptor Tyrosine Kinase and a Possible Mechanism of its Activation by EGF, *J. Biol. Chem. 267*, 20638−20647.
18. Parast, C. V., Mroczkowski, B., Pinko, C., Misialek, S., Khambatta, G., and Appelt, K. (1998) Characterization of the Kinetic Mechanism of the Catalytic Domain of Human Vascular Endothelial Growth Factor Receptor-2 Tyrosine Kinase (VEGFR2 TK), a Key Enzyme in Angiogenisis, *Biochemistry 37*, 16788−16801.
19. Murray, B. W., Padrique, E. S., Pinko, C., and McTigue, M. A. (2001) Mechanistic Effects of Autophosphorylation on Receptor Tyrosine Kinase Catalysis: Enzymatic Characterization of Tie2 and Phospho-Tie2, *Biochemistry 40*, 10243−10253.

20. Hays, J. L., and Watowich, S. J. (2003) Oligomerization-induced Modulation of the TPR-MET Tyrosine Kinase Activity, *J. Biol. Chem. 278*, 27456−27463.
21. Mol, C. D., Lim, K. B., Sridhar, V., Zou, H., Chien, E. Y. T., Sang, B., Nowakowski, J., Kassel, D. B., Cronin, C. N., and McRee, D. E. (2003) Structure of the c-Kit Product Complex Reveals the Basis for Kinase Transactivation, *J. Biol. Chem. 278*, 31461−31464.
22. Stamos, J., Sliwkowski, M. X., and Eigenbrot, C. (2002) Structure of the Epidermal Growth Factor Receptor Kinase Domain Alone and in Complex with a 4-Anilinoquinazoline Inhibitor, *J. Biol. Chem. 277*, 46265−46272.
23. Cheng, K., and Koland, J. G. (1998) Nucleotide Binding Properties of Kinase-Deficient Epidermal Growth Factor Receptors, *Biochem. J. 330*, 353−359.
24. Beebe, J. A., Wiepz, G. J., Guardarrama, A. G., Bertics, P. J., and Burke, T. J. (2003) A Carboxy Terminal Mutation of the EGF Receptor Alters Tyrosine Kinase Activity and Substrate Specificity As Measured by Fluorescence Polarization Assay, *J. Biol. Chem. 278*, 26810−26816.
25. Kohanski, R. A. (1993) Insulin Receptor Autophosphorylation. I. Autophosphorylation Kinetics of the Native Receptor and Its Cytoplasmic Kinase Domain, *Biochemistry 32*, 5766−5772.
26. Cooper, C. S., Park, M., Blair, D. G., Tainsky, M. A., Huebner, K., Croce, C. M., and Vande Woode, G. F. (1984) Molecular Cloning of a New Transforming Gene from a Chemically Transformed Human Cell Line, *Nature 311*, 29−33.
27. Bangs, P. L., Sparks, C. A., Odgren, P. R., and Fey, E. G. (1996) Product of the Oncogene Activating Gene *Tpr* is a Phosphorylated Protein of the Nuclear Pore Complex, *J. Cell. Biochem. 61*, 48−60.
28. Liang, T. J., Reid, A. E., Xavier, R., Cardiff, R. D., and Wang, T. C. (1996) Transgenic Expression of Tpr-Met Oncogene Leads to Development of Mammary Hyperplasia and Tumors, *J. Clin. Invest. 97*, 2872−2877.
29. Fixman, F. D., Naujokas, M. A., Rodrigues, G. A., Moran, M. F., and Park, M. (1995) Efficient Cell Transformation by the TPR-MET Oncoprotein is Dependent Upon Tyrosine 489 in the Carboxy Terminus, *Oncogene 10*, 237−249.
30. Jeffers, M., Koochekpour, S., Fiscella, M., Sathyanarayana, B. K., and Van de Woude, G. F. (1998) Signaling Requirements for Oncogenic Forms of the cMET Tyrosine Kinase Receptor, *Oncogene 17*, 2691−2700.
31. Sattler, M., Pride, Y. B., Ma, P., Gramlich, J. L., Chu, S. C., Quinnan, L. A., Shirazian, S., Liang, C., Podar, K., Christensen, J. G., and Salgia, R. (2003) A Novel Small Molecule Met Inhibitor Induces Apoptosis in Cells Transformed by the Oncogenic TPR-MET Tyrosine Kinase, *Cancer Res. 63*, 5462−5469.
32. Xiao, G. H., Jeffers, M., Bellacosa, A., Mitsuuchi, Y., Vande Woude, G. F., and Testa, J. R. (2001) Anti-apoptotic Signaling by Hepatocyte Growth Factor/Met via the Phosphatidylinositol 3-kinase/Akt and Mitogen-Activated Protein Kinase Pathways, *Proc. Natl. Acad. Sci. U.S.A. 98*, 247−252.
33. Hiratsuka, T. (1983) New Ribose-Modified Fluorescent Analogs of Adenine and Guanine Nucleotides Available as Substrates for Various Enzymes, *Biochim. Biophys. Acta 742*, 496−508.
34. Fattori, D., Urbani, A., Brunetti, M., Ingenito, R., Pessi, A., Prendergrast, K., Narjes, F., Matassa, V., De Francesco, R., and Steinkuhler, C. (2000) Probing the Active Site of the Hepatitis C Virus Serine Protease by Fluorescence Resonance Energy Transfer, *J. Biol. Chem. 275*, 15106−15113.
35. Hubbard, S. R. (1997) Crystal Structure of the Activated Insulin Receptor Tyrosine Kinase in Complex with Peptide Substrate and ATP Analog, *EMBO J. 16*, 5573−5581.
36. Ni, D. Q., Shaffer, J., and Adams, J. A. (2000) Insight into Nucleotide Binding on Protein Kinase A using Fluorescent Adenosine Derivatives, *Protein Sci. 9*, 1818−1827.
37. Cheng, K., and Koland, J. G. (1996) Nucleotide Binding by the Epidermal Growth Factor Receptor Protein Tyrosine Kinase, *J. Biol. Chem. 271*, 311−318.
38. Shaffer, J., Sun, G., and Adams, J. A. (2001) Nucleotide Release and Associated Conformational Changes Regulate Function in the COOH-Terminal Src Kinase, Csk, *Biochemistry 40*, 11149−11155.
39. Naldini, L., Vigna, E., Ferracini, R., Longati, P., Gandino, L., Prat, M., and Comoglio, P. (1991) The Tyrosine Kinase Encoded by the MET Proto-oncogene is Activated by Autophosphorylation, *Mol. Cell. Biol. 13*, 1793−1803.
40. Rodrigues, G. A., and Park, M. (1994) Autophosphorylation Modulates the Kinase Activity and Oncogenic Potential of the Met Receptor Tyrosine Kinase, *Oncogene 9*, 2019−2027.
41. Bardelli, A., Longati, P., Williams, T. A., Benvenuti, S., and Comoglio, P. M. (1999) A Peptide Representing the Carboxy Terminal Tail of the MET Receptor Inhibits Kinase Activity and Invasive Growth, *J. Biol. Chem. 274*, 29274−29281.
42. Filipek, A., and Soderling, T. R. (1993) Identification of an Autoinhibitory Domain in the Insulin Receptor Tyrosine Kinase, *Mol. Cell. Biochem. 120*, 103−110.
43. Shimizu, A., Perrson, C., Heldin, C. H., and Ostman, A. (2001) Ligand Stimulation Reduces the Platelet Derived Growth Factor Receptor Susceptibility to Tyrosine Dephosphorylation, *J. Biol. Chem. 276*, 27749−27752.

BI0363275